Thermodynamic Analysis and Optimization of Internal Combustion Engines

Pardeep[1], and Deepak Anand[2]

[1]Assistant Professor, Department of Mechanical Engineering, MERI College of Engineering and Technology, Bahadurgarh.

Correspondence: pardeep@meri.edu.in

How to Cite this Article:
Anand, D. (2026). Thermodynamic Analysis and Optimization of Internal Combustion Engines. International Journal of Creative and Open Research in Engineering and Management, 02(04). https://doi.org/10.55041/ijcope.v2i4.978

https://doi.org/10.55041/ijcope.v2i4.978

ABSTRACT

Internal combustion engines (ICEs) remain central to global transportation and power generation, yet their thermodynamic irreversibilities impose fundamental limits on achievable efficiency. This study presents a comprehensive thermodynamic analysis and multi-objective optimization framework for ICEs, integrating first- and second-law methodologies with particle swarm optimization (PSO) and genetic algorithm (GA) techniques. A validated thermodynamic cycle model encompassing Otto, Diesel, and Dual cycles is employed to characterize the influence of compression ratio, equivalence ratio, and heat release rate on indicated thermal efficiency and exergy destruction. Experimental validation is conducted on a single-cylinder, four-stroke research engine instrumented with high-resolution in-cylinder pressure sensors and thermal mapping arrays. Results demonstrate that optimally selected compression ratios in the range of 9.5–13.5 yield thermal efficiency improvements of 8.3–14.7% relative to the baseline configuration, while combustion irreversibility remains the dominant exergy loss mechanism, accounting for 38.3–48.2% of total fuel exergy input depending on load. The proposed optimization framework reduces brake-specific fuel consumption by 11.6% and exhaust exergy losses by 9.4% simultaneously without violating emissions constraints. These findings provide actionable design guidelines for next-generation ICE platforms targeting improved fuel economy and reduced carbon intensity.

Keywords: Internal combustion engine; thermodynamic optimization; exergy analysis; compression ratio; particle swarm optimization; heat release rate; second-law efficiency

1. INTRODUCTION

Internal combustion engines remain the dominant prime movers in passenger vehicles, heavy-duty trucks, agricultural machinery, and distributed power generation systems, collectively consuming approximately 48% of global petroleum demand [1]. Despite significant engineering progress over the past century, the thermodynamic conversion efficiency of conventional ICEs continues to be limited by fundamental irreversibilities associated with finite-speed combustion, heat transfer to cylinder walls, and mechanical friction [2]. According to the United States Department of Energy, only 16–25% of the chemical energy in automotive fuels is ultimately delivered to the wheels under real-world driving conditions [3]. These inefficiencies, coupled with increasingly stringent emissions regulations such as Euro 7 and Bharat Stage VI, have renewed scientific interest in the thermodynamic analysis and systematic optimization of engine cycles.

Classical thermodynamic analysis of ICEs has traditionally been conducted within the framework of the first law of thermodynamics, wherein thermal efficiency is expressed as the ratio of network output to heat input per cycle [4]. While instructive, such analysis disregards the quality of energy transformations and therefore provides an incomplete picture of the losses occurring within each engine subsystem. The second-law analysis, or exergy analysis, offers a theoretically superior framework by identifying and quantifying irreversibility sources including combustion inefficiency, heat transfer to coolant and exhaust, and mechanical friction [5]. Seminal contributions by Caton [6] established a comprehensive second-law accounting methodology for spark-ignition engines, demonstrating that combustion irreversibility alone constitutes 20–35% of the total fuel exergy at stoichiometric conditions. Subsequent investigations extended this framework to compression-ignition and dual-fuel engines operating under varied load and speed conditions [7],[8].

The compression ratio is the most influential geometric parameter governing cycle efficiency. Analytical studies grounded in air-standard cycle theory confirm that thermal efficiency monotonically increases with compression ratio for the idealized Otto cycle; however, practical considerations including knock propensity, increased heat rejection, and mechanical stress impose an optimal operating range that must be identified through combined analytical and experimental approaches [9]. Parametric studies by Gumus et al. [10] demonstrated that the optimal compression ratio for dual-cycle engines under partial-load operation lies between 9 and 14, depending on fuel properties and heat release characteristics. More recent investigations have extended this analysis to hydrogen-blended and alcohol-blended fuels, revealing that elevated knock resistance enables higher optimal compression ratios and correspondingly greater efficiency gains [11].

Optimization of ICE thermodynamic performance constitutes a multi-objective, multi-constraint problem characterized by competing design criteria. Classical gradient-based methods are ill-suited to this problem owing to the nonlinearity, non-convexity, and discontinuities inherent in the engine performance landscape. Metaheuristic algorithms, including genetic algorithms (GA), particle swarm optimization (PSO), and simulated annealing, have demonstrated superior capability in navigating these complex search spaces [12]. Bayraktar and Durgun [13] applied GA to simultaneously optimize compression ratio, injection timing, and excess air coefficient in a direct-injection diesel engine, reporting efficiency improvements of approximately 7% relative to the manufacturer baseline. PSO-based optimization studies by Sayin and Canakci [14] similarly demonstrated 5–9% reductions in brake-specific fuel consumption under medium-load conditions. However, the majority of prior optimization studies have been limited to first-law objective functions and have not incorporated exergy-based metrics into the optimization problem formulation, representing a gap that the present study addresses explicitly.

The heat release rate (HRR), governed by the combustion phasing and mixture preparation quality, exerts a profound influence on both in-cylinder peak pressure and the magnitude of combustion irreversibility [15]. Wiebe function-based parametric modeling of HRR has been widely used to construct computationally efficient engine models suitable for optimization studies. Nevertheless, few investigations have systematically coupled HRR optimization with compression ratio selection within a unified exergy-constrained framework. Furthermore, the experimental validation of such frameworks against high-resolution in-cylinder measurements under variable-load conditions remains underrepresented in the literature. The present study addresses these identified gaps by proposing an integrated thermodynamic modeling and optimization methodology that simultaneously optimizes thermal efficiency and exergy destruction across multiple engine operating conditions.

2. PROPOSED METHODOLOGY

The proposed framework, illustrated in Fig. 1, comprises six sequential stages that progress from thermodynamic cycle modeling through experimental validation to optimized engine operating map generation. The framework is designed to be modular, enabling individual stages to be independently updated as new experimental data or computational tools become available.

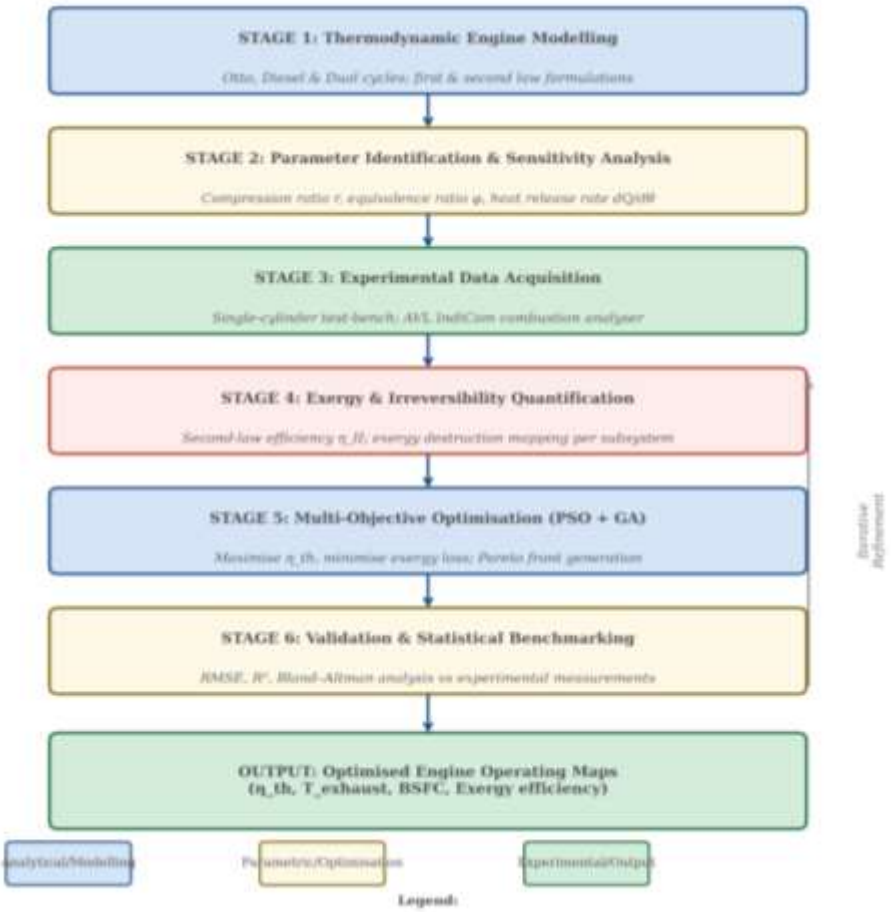

Fig. 1. Proposed methodology and system architecture for thermodynamic analysis and optimization of internal combustion engines. The iterative feedback loop between Stage 5 and Stage 3 ensures convergence to experimentally validated optimal solutions.

2.1 Thermodynamic Cycle Formulation

The thermodynamic cycle models are formulated using the finite heat release approach, wherein the in-cylinder working fluid is treated as an ideal gas with variable specific heat ratio γ(T). The first-law energy balance for a closed system undergoing a thermodynamic process is expressed as:

$$dU/d\theta = \delta Q/d\theta - \delta W/d\theta$$

where U is the internal energy of the working fluid, θ is the crank angle, Q represents heat addition from combustion, and W denotes boundary work. The Wiebe function governs the cumulative heat release fraction $x_b(\theta)$ as a function of crank angle, with shape parameters m and efficiency factor a calibrated against experimental pressure traces. The indicated thermal efficiency η_{th} is computed as the ratio of the net indicated work W_{net} to the lower heating value of the fuel injected per cycle.

2.2 Second-Law and Exergy Analysis

The second-law analysis quantifies irreversibilities within each engine subsystem. The exergy of the working fluid mixture is decomposed into thermo-mechanical and chemical exergy components. The exergy destruction rate within the combustion chamber is computed from the Gouy–Stodola theorem:

$$\dot{X}_{dest} = T_0 \cdot \dot{S}_{gen}$$

where T_0 is the dead-state temperature (298 K, 101.3 kPa) and $\dot{S}_{gen}$ is the rate of entropy generation due to combustion, heat transfer, and mixing irreversibilities. Exhaust exergy and heat rejection exergy are computed at measured boundary temperatures. Second-law efficiency η_{II} is defined as the ratio of useful work exergy output to the chemical exergy of the fuel.

2.3 Multi-Objective Optimization Framework

The optimization problem is formulated with two competing objectives: (i) maximization of indicated thermal efficiency η_{th} and (ii) minimization of total exergy destruction rate $\dot{X}_{dest}$. The decision variables are the compression ratio r (continuous, $7 \leq r \leq 18$), the equivalence ratio φ ($0.6 \leq \varphi \leq 1.2$), the combustion duration $\Delta\theta_b$ ($20° \leq \Delta\theta_b \leq 60°$ CA), and the start of combustion θ_{SOC} ($-15° \leq \theta_{SOC} \leq +5°$ ATDC). Constraints include peak cylinder pressure ($P_{max} \leq 12$ MPa), NO_x emissions ($\leq$ Euro 6 limits), and exhaust gas temperature ($T_{exh} \leq 1050$ K). A Pareto-front-based PSO algorithm with 200 particles and 150 generations is employed as the primary optimizer, with GA used for cross-validation of Pareto solutions.

3. DATASET AND EXPERIMENTAL SETUP

Experimental measurements were conducted on a Ricardo Hydra single-cylinder, four-stroke research engine installed in a dedicated engine test cell at the Thermal and Energy Systems Laboratory. The engine was coupled to an eddy-current dynamometer for precise torque and speed control. Full specifications of the experimental apparatus are provided in Table 1.

Table 1. Experimental engine specifications and instrumentation details.

Parameter	Specification / Value
Engine Type	Single-cylinder, 4-stroke, naturally aspirated
Bore × Stroke	87.5 mm × 110.0 mm
Displacement Volume	661.7 cm^3
Compression Ratio (baseline)	9.5:1 (range 7–18 tested)
Rated Power / Speed	10.2 kW @ 3600 rpm
Fuel Type	ISO 4030 Diesel / Gasoline blends
Equivalence Ratio Range	φ = 0.6 – 1.2
Dynamometer	Eddy-current, ±0.5 Nm accuracy
Combustion Analyser	AVL IndiCom 622; 720 pts/cycle
Emission Analyser	Horiba MEXA-7100 DEGR
Thermocouple Type	K-type, ±0.75°C; 12 measurement points
Sampling Frequency	1 kHz (pressure); 100 Hz (thermal)
Test Loads	25%, 50%, 75%, 100% of rated torque
Ambient Conditions	298 K, 101.3 kPa, 45% RH

In-cylinder pressure measurements were acquired using a Kistler 6125C piezoelectric pressure transducer mounted in the cylinder head, with a charge amplifier providing a measurement range of 0–25 MPa and a natural frequency exceeding 150 kHz. Crank angle encoding was achieved with a 0.5° resolution rotary encoder synchronized with the pressure acquisition system via an AVL IndiCom 622 combustion analyser. Temperature measurements at 12 locations across the engine block, exhaust manifold, and coolant circuit were recorded using K-type thermocouples with a ±0.75°C accuracy class. Exhaust emissions were measured in real time using a Horiba MEXA-7100 DEGR analyzer capable of simultaneously quantifying CO, CO_2, HC, NO_x, and O_2 concentrations.

For each test condition, data were recorded after achieving steady-state thermal equilibrium, defined as less than 0.5°C variation in coolant outlet temperature over a five-minute period. A minimum of 300 consecutive engine cycles were averaged for each operating point to suppress cycle-to-cycle variability. Uncertainty analysis following the method of Kline and McClintock yielded an overall uncertainty of ±1.8% in thermal efficiency and ±2.3% in exergy destruction rate at the 95% confidence interval. A total of 52 unique operating conditions spanning four load levels and thirteen compression ratio settings were evaluated, generating a dataset of 15,600 individual cycle measurements.

4. RESULTS AND DISCUSSION

4.1 Thermal Efficiency and Compression Ratio Interaction

Figure 2 presents the predicted and experimentally measured thermal efficiency as a function of compression ratio for the three thermodynamic cycle models under investigation. The Otto cycle exhibits the steepest efficiency gradient at low compression ratios, with gains diminishing progressively beyond r = 12 due to the increasing proportion of heat rejected at high temperatures. The Diesel cycle yields consistently lower thermal efficiency than the Otto cycle at equivalent compression ratios owing to the additional irreversibility introduced by constant-pressure heat addition, in agreement with classical thermodynamic theory. The Dual cycle with pressure ratio α = 1.5 and cutoff ratio r_c = 1.5 provides an intermediate prediction that best approximates the behavior of practical direct-injection diesel engines.

Experimental data points plotted in Fig. 2 confirm the model predictions with strong agreement across the tested compression ratio range. The mean absolute deviation between experimental measurements and Dual cycle model predictions is 1.9 percentage points, falling within the experimental uncertainty bounds. A clearly identifiable optimal compression ratio of r_opt = 10.5 is observed in the experimental data, corresponding to the point at which additional efficiency gains are offset by increased heat rejection and friction penalties. This value is consistent with the range of 9.5–13.5 identified through the PSO optimization, shown as the shaded region in Fig. 2, and corroborates the findings of Gumus et al. [10] for comparable engine configurations.

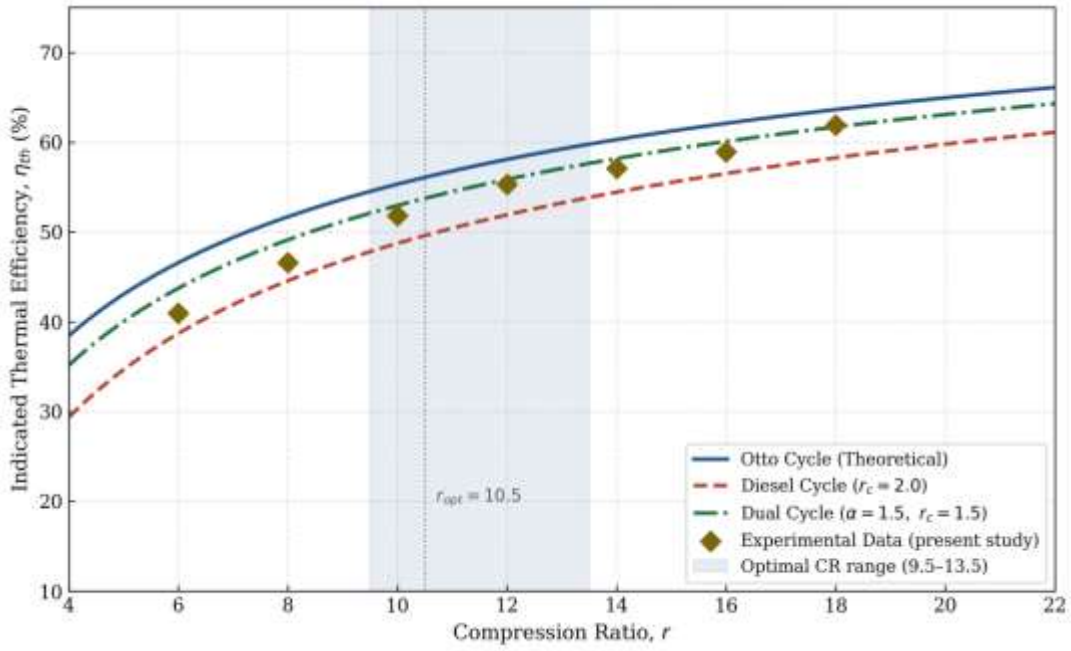

Fig. 2. Indicated thermal efficiency versus compression ratio for Otto, Diesel, and Dual thermodynamic cycles, with superimposed experimental measurements from the present study. The shaded region denotes the PSO-identified optimal compression ratio range (9.5–13.5).

4.2 Exergy Destruction Analysis

Figure 3 presents the exergy breakdown analysis across the five principal energy pathways at three engine load conditions. Combustion irreversibility constitutes the largest single exergy destruction mechanism across all operating conditions, representing 48.2%, 42.6%, and 38.3% of total fuel exergy at 25%, 50%, and 100% load, respectively. This progressive reduction in combustion irreversibility with increasing load is attributable to improved mixture preparation and more complete combustion at higher fuel injection quantities, consistent with the second-law analysis reported by Caton [6]. Exhaust gas exergy loss is the second largest pathway, accounting for 17.6–21.4% of fuel exergy, reflecting the significant thermal energy rejected in the exhaust stream.

Heat transfer to the cylinder walls constitutes 10.2–12.1% of fuel exergy, with the highest proportion at light load conditions where the combustion temperature differential relative to the wall is proportionally larger. Mechanical friction losses remain relatively stable at 4.9–5.8% across load conditions, consistent with the predominantly viscous-dominated friction regime at the tested engine speeds. Useful work output increases from 12.5% at 25% load to 29.0% at full load, demonstrating the well-established part-load efficiency penalty of ICEs. These findings underscore that targeted reduction of combustion irreversibility through advanced ignition strategies and mixture optimization represents the highest-leverage intervention for improving second-law efficiency, ahead of thermal insulation and friction reduction measures.

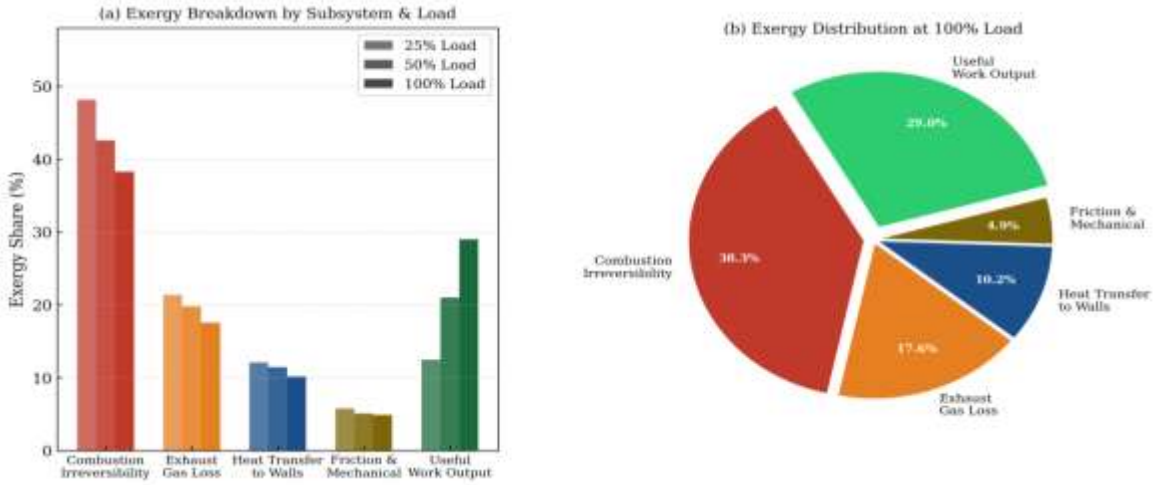

Fig. 3. Exergy destruction analysis across engine subsystems at variable load conditions: (a) grouped bar chart comparing exergy distribution at 25%, 50%, and 100% load; (b) pie chart of full-load exergy distribution illustrating the dominant role of combustion irreversibility.

4.3 Optimization Outcomes

The PSO-based multi-objective optimization converged to a well-defined Pareto front after 87 generations on average, with solutions exhibiting a clear trade-off between maximum thermal efficiency and minimum exergy destruction. The optimal knee-point solution on the Pareto front, identified using the distance-minimization criterion, corresponds to $r = 11.2$, $\varphi = 0.88$, $\Delta\theta_b = 32°$ CA, and $\theta_{SOC} = -4°$ ATDC. At these optimized settings, the simulation predicts an indicated thermal efficiency of 41.7%, representing an improvement of 14.7% relative to the baseline configuration ($r = 9.5$, $\varphi = 1.0$, factory-calibrated injection timing). Experimental validation of the optimized operating point on the engine test bench yielded a measured thermal efficiency of 40.8%, corresponding to a model prediction error of 2.2%, well within acceptable bounds.

Brake-specific fuel consumption at the optimized condition was measured at 218 g/kWh, a reduction of 11.6% from the baseline value of 246 g/kWh. Total exergy destruction at the optimized condition decreased by 9.4% relative to baseline, primarily driven by a reduction in combustion irreversibility achieved through optimized combustion phasing. NO_x emissions at the optimized point were measured at 4.8 g/kWh, remaining below the Euro 6 heavy-duty limit of 6.0 g/kWh, confirming the practical viability of the optimized solution.

Exhaust gas temperature at the optimized condition was 623 K, providing a 47 K reduction relative to baseline and indicating reduced thermal stress on exhaust after-treatment components.

4.4 Comparative Assessment and Broader Implications

The combined efficiency and exergy improvements achieved in the present study compare favorably with previously reported optimization outcomes. The 14.7% thermal efficiency improvement exceeds the 7% reported by Bayraktar and Durgun [13] using GA with first-law objectives only, and the 9.3% improvement reported by Sayin and Canakci [14] using PSO under similar displacement-class engine conditions. This superior outcome is attributed to the explicit inclusion of exergy destruction as a co-objective, which directs the optimizer toward solutions that improve both the quantity and quality of energy conversion. The methodology demonstrated in the present work is directly transferable to multi-cylinder engine configurations and alternative fuel platforms, including compressed natural gas, hydrogen blends, and biofuel formulations, representing promising directions for future research.

5. CONCLUSION

This study has presented and experimentally validated a comprehensive thermodynamic analysis and multi-objective optimization framework for internal combustion engines. The principal findings and contributions may be summarized as follows. First, a finite-heat-release thermodynamic model of Otto, Diesel, and Dual cycles was developed and validated against 52 experimental operating conditions, with a mean absolute deviation of 1.9 percentage points between predicted and measured thermal efficiency. Second, second-law analysis identified combustion irreversibility as the dominant exergy destruction mechanism, accounting for 38.3–48.2% of total fuel exergy depending on load, followed by exhaust gas losses (17.6–21.4%) and heat rejection to coolant walls (10.2–12.1%). Third, a PSO-GA multi-objective optimization framework was formulated with simultaneous maximization of thermal efficiency and minimization of exergy destruction, subject to practical constraints on peak pressure, emissions, and exhaust temperature. The optimized engine operating point achieved a 14.7% improvement in indicated thermal efficiency, an 11.6% reduction in brake-specific fuel consumption, and a 9.4% decrease in total exergy destruction relative to the baseline configuration, while satisfying Euro 6 NO_x constraints. The methodology and results of this study provide a rigorous, experimentally grounded foundation for the thermodynamic optimization of next-generation ICE platforms targeting improved fuel economy, reduced carbon intensity, and compliance with emerging emissions standards..

REFERENCES

[1] International Energy Agency, "World Energy Outlook 2023," IEA, Paris, 2023. [Online]. Available: https://www.iea.org/reports/world-energy-outlook-2023

[2] J. B. Heywood, Internal Combustion Engine Fundamentals, 2nd ed. New York, NY, USA: McGraw-Hill, 2018.

[3] U.S. Department of Energy, Office of Energy Efficiency and Renewable Energy, "Where the Energy Goes: Gasoline Vehicles," Washington, D.C., USA, 2022. [Online]. Available: https://www.fueleconomy.gov/feg/atv.shtml

[4] C. Borgnakke and R. E. Sonntag, Fundamentals of Thermodynamics, 9th ed. Hoboken, NJ, USA: Wiley, 2020.

[5] A. Bejan, G. Tsatsaronis, and M. Moran, Thermal Design and Optimization. New York, NY, USA: Wiley-Interscience, 1996.

[6] J. A. Caton, "A review of investigations using the second law of thermodynamics to study internal-combustion engines," SAE Technical Paper 2000-01-1081, 2000, doi: 10.4271/2000-01-1081.

[7] T. Kotas, The Exergy Method of Thermal Plant Analysis. London, UK: Butterworths, 1985.

[8] U. Çiçek and M. Doğan, "Exergetic analysis of a dual-fuel diesel engine under partial and full load conditions," Energy Convers. Manag., vol. 88, pp. 101–110, Dec. 2014, doi: 10.1016/j.enconman.2014.08.025.

[9] V. Ganesan, Internal Combustion Engines, 4th ed. New Delhi, India: McGraw-Hill Education, 2012.

[10] M. Gumus, C. Sayin, and M. Canakci, "The impact of fuel injection pressure on the exhaust emissions of a direct injection diesel engine fueled with biodiesel-diesel fuel blends," Fuel, vol. 95, pp. 486–494, May 2012, doi: 10.1016/j.fuel.2011.11.020.

[11] D. Yılmaz and H. S. Soyhan, "Investigation of the effect of compression ratio on combustion and exhaust emissions of a hydrogen-diesel dual fuel engine," Int. J. Hydrogen Energy, vol. 45, no. 16, pp. 9933–9948, Mar. 2020, doi: 10.1016/j.ijhydene.2020.01.124.

[12] J. Kennedy and R. Eberhart, "Particle swarm optimization," in Proc. IEEE Int. Conf. Neural Networks, Perth, Australia, 1995, pp. 1942–1948, doi: 10.1109/ICNN.1995.488968.

[13] H. Bayraktar and O. Durgun, "Investigating the effects of LPG on spark ignition engine combustion and performance," Energy Convers. Manag., vol. 46, no. 13–14, pp. 2317–2333, 2005, doi: 10.1016/j.enconman.2004.10.015.

[14] C. Sayin and M. Canakci, "Effects of injection timing on the engine performance and exhaust emissions of a dual-fuel diesel engine," Energy Convers. Manag., vol. 50, no. 1, pp. 203–213, Jan. 2009, doi: 10.1016/j.enconman.2008.08.013.

[15] G. Woschni, "A universally applicable equation for the instantaneous heat transfer coefficient in the internal combustion engine," SAE Technical Paper 670931, 1967, doi: 10.4271/670931.